BUILDING RESEARCH JOURNAL
VOLUME 60, 2012 NUMBER 1 – 2

TURBULENCES IN ARTIFICIAL BOUNDARY LAYER OF PHOTOVOLTAIC POWER PLANTS

ALEXANDER TESAR

The aeroelastic assessment of turbulences appearing in artificial boundary layer of photovoltaic power plants is treated in the present paper. The approach suggested takes into account multiple functions in the analysis of skew flat plates of solar panels subjected to laminar and turbulent wind forcing. Analysis and experimental assessments in the aerodynamic tunnel are presented. Some results obtained are discussed.

Keywords: aerodynamic tunnel, aeroelasticity, artificial boundary layer, photovoltaic power plant, mechanics of turbulent wind motion, skew flat plate, solar panel, turbulences, wave propagation

1. Introduction

The modeling of the turbulent air flow in aerodynamic tunnels is a research domain based on advanced scientific technologies. They are imposed, for example, by the necessity of studying the turbulent air movement in the proximity of photovoltaic power plants treated in this paper. Due to the testing of models in aerodynamic tunnels the modern codes for design of structures exposed to the wind turbulences are able to assess in a highly accurate degree the effect of these actions. The models of turbulent air flow are used in the assessments being validated by tunnel testing measurements of the parameters integrated in the calculation.

The topic of present paper is the assessment of ultimate aeroelastic behaviour of skew plates of solar panels in photovoltaic power plants subjected to laminar and turbulent forcing of wind (see Fig. 1). The skew flat plates of solar panels are supported by metal structures anchored into terrain. The panels create the active fields of the power plants studied. The photovoltaic power plants are located in territories where the wind loads represent the dominant environmental forcing. The forcing is to be unified into maximal design values for given territory. All structural elements are to be designed in accordance with valid standards and their aeroelastic assessments are required, for example, due to the recommendations of the EUROCODE 1, Loads on Structures, Part 1.4, General Loads, and Wind Loads.

Institute of Construction and Architecture, Slovak Academy of Sciences, Dubravska cesta 9, 845 03 Bratislava 45, Slovak Republic, e-mail: usarate@savba.sk

Active fields of photovoltaic power plants with a multitude of flat plates with solar panels create an artificial boundary layer with laminar and turbulent wind forcing. The aeroelastic response depends on the following options:

- wind speed,
- wind direction,
- wind flow (laminar or turbulent),
- wind temperature and humidity,
- snow and ice loads,
- gaps between solar panels,
- geometry and configuration of active fields of solar panels,
- properties of all structural elements.

Because of the small height of solar panels above the terrain there occur the cataract air flows on edges of the flat plates which increase the wind speeds and pressures. Regarding the variability of configurations of photovoltaic power plants with artificial boundary layer in small heights, there appear the turbulent wind flows measurable only in the wind tunnel. The measurements in aerodynamic tunnels submit the data required for the analysis of the problem.

2. Analysis

The idea of application of the flat plate aerodynamics in the field of preliminary structural design was introduced by Bleich (1950). Selberg (1961, 1966) and Hjorth-Hansen (1966) carried out an experimental investigation of a number of cross-sections presented an approximate expression for the flutter velocity of a plate acted upon by Theodorsen´s forces (1935). In their contribution Klöppel and Weber (1963) employed the flat plate stability limit as a reference quantity in the same way as Selberg. A general solution of the flat plate equations for a linear model was given by Frandsen (1966). Frandsen showed that a simplified expression by Rocard (1965) for the limit state stability of bridges turned out to be a good approximation for the flat plate flutter velocity. Scruton (1965) pointed to the apparent similarities of the behaviour of realistic models and flat plate computational model. Buffeting appearing by some forcing conditions was the topic of research of Davenport (1962). Bridge deck flutter derivatives and their action in general aeroelasticity were treated by Scanlan and coworkers (1971, 1974, 1971 and 1966). Some aspects of non-stationary airfoil theory were dealt with by Sears (1941). Significant research results concerning the problem are contained also in Refs 15 – 21.

Slender structures of skew flat plates of photovoltaic power plants are prone to wind-induced vibrations for various reasons. Some issues considered in their wind resistant design are mentioned by:

1. Wind turbulences force the plate with a considerable power and the forced movements owing to turbulence and associated mechanisms are stochastic in nature.
2. There can be produced a strong vortex wake associated with aerodynamic drag force experienced by the plate. Depending on wind speed and cross-section's shape, the shedding of vortices is more or less regular with shedding periods inversely proportional to the wind speed. In resonance conditions the structure's oscillation can control the rhythm of the vortex shedding.
3. Aside the known vortex trail type excitation the more general types of forcing appear in the plate. The possible re-attachment of separated flow, the vortices generated by the local geometry and movement of the plate contribute to such periodic forcing.
4. Aeroelastic forces proportional to the movement of the plate can produce self-induced divergent vibrations at some wind speeds.

5. In the design of the plate it is to be avoided that absolute value of negative aerodynamic damping exceeds the positive mechanical damping producing across-wind flexural mode instability. Associated critical wind speed is the flutter velocity while corresponding circular frequency is the flutter frequency.
6. At the onset of divergence the aerodynamic instability of the plate is initiated.

In this paper the wind induced structural phenomena are treated by transient dynamics (Tanaka, H., 1992 and Tesar, A., 1988). Laminar and turbulent wind forcing is studied adopting the wave propagation approach (Tesar, A., 1993). The goal is to develop the approach based on transient dynamics combined with wave propagation forcing and adopted for the analysis of aeroelastic response of skew flat plates of photovoltaic power plants on the basis of results obtained in scope of experimental testing in the wind tunnel (Juhásová, E., Motlík I., Vrabec, M., 1998 and STN EN 1991-1-4 Eurocode 1.).

3. Ultimate behaviour

The skew plates of photovoltaic power plants are exposed to low frequency vibrations initiated by wind. Such forcing causes the vibrations due to the von Kármán vortices occurring with frequencies close to resonance behaviour. The photovoltaic power plants are created by active fields of photovoltaic panels positioned close together. There is created the artificial boundary layer having variable parameters due to orography, direction and velocity of the wind. The aeroelastic assessment is made by the analysis of turbulences modeled by waves in the air flow. For the analysis the FETM-approach is suggested as a combination of the finite element and transfer matrix techniques (Juhásová, E., Motlík I., Vrabec, M., 1998 and Tesar, A. and Svolik, J. 1993).

The models of turbulent air flow are used in assessments being validated by tunnel testing measurements of the parameters integrated in the analysis (Juhásová, E., Motlík I., Vrabec, M., 1998) due to valid codes (STN EN 1991-1-4 Eurocode 1.). The nonlinear time response is made by energy approach suggested in Refs. (Tesar, A. and Tvrda, K., 2006 and 2007).

4. Mechanics of turbulent motion

All turbulences in the wind forcing are considered as a special family of motions from one space region into another one. Their updated configuration is specified by location of the air displacements in space and time. The variations of configurations are continuous and during deformation there appear no new boundary conditions. Each new configuration is related to a reference position stated.

When taking into account the Cartesian coordinates *x, y, z* and corresponding displacements *u, v, w,* the Green strain tensor is given by

$$E_{xx} = \partial u_x/\partial x + [(\partial u_x/\partial x)^2 + (\partial u_y/\partial y)^2 + (\partial u_z/\partial z)^2]/2, \quad (1)$$

$$E_{xy} = [(\partial u_y/\partial x) + (\partial u_x/\partial y) + (\partial u_x/\partial x)(\partial u_x/\partial y) + (\partial u_y/\partial x)(\partial u_y/\partial y) + (\partial u_z/\partial x)(\partial u_z/\partial y)]/, \quad (2)$$

..., etc.

In order to set up the constitutive equations, the stress tensor with the same reference is needed. The second Piola-Kirchhoff stress tensor S_{ij} has the properties required and the generalized equation of the air flow is given by

$$S_{ij} = g(E_{ij}), \tag{3}$$

with g as a function of the Green strain tensor E_{ij}.

When analysing the air flow with volume, surface area and density, B, S and $r_{o,}$ respectively, the volume forces of the mass unit are given by $F_{o,i}$ and strains by T_i. The system in equilibrium is submitted to a virtual displacement du_i being kinematically consistent with initial conditions assumed. The equilibrium of the virtual work is given by

$$\int S_{ij}\, \delta E_{ij}\, dB - \int T_i\, \delta u_i\, dS - \int P_i \delta u_i\, dB = 0, \tag{4}$$

with substitution

$$P_i = \rho_o\, F_{o,i}. \tag{5}$$

Equation (4) specifies the stationary value of the potential energy in all deformations u_i. The incremental equivalent of corresponding variation principle is given by

$$\int S_{ij}^{(1)}\, \delta E_{ij}^{(1)}\, dB - \int T_i^{(1)}\, du_i^{(1)}\, dS - \int P_i^{(1)}\, \delta u_i^{(1)}\, dB = 0, \tag{6}$$

$$\int S_{ij}^{(2)}\, \delta E_{ij}^{(2)}\, dB - \int T_i^{(2)}\, du_i^{(2)}\, dS - \int P_i^{(2)}\, \delta u_i^{(2)}\, dB = 0, \tag{7}$$

with superscripts (1) and (2) for neighbouring configurations studied. The strains and volume forces have the same reference configuration and there holds

$$\Delta T_i = T_i^{(2)} - T_i^{(1)}, \tag{8}$$

$$\Delta P_i = P_i^{(2)} - P_i^{(1)}, \tag{9}$$

The variations of the both deformation fields are the same

$$\delta u_i = \delta u_i^{(1)} = \delta u_i^{(2)}. \tag{10}$$

The incremental virtual work equation is given by Eqs. (6) and (7) as

$$\int (S_{ij}^{(2)}\, \delta E_{ij}^{(2)} - S_{ij}^{(1)}\, \delta E_{ij}^{(1)})\, dB - \int \Delta T_i\, \delta u_i\, dS - \int \Delta P_i\, \delta u_i\, dB = 0, \tag{11}$$

when taking into account the virtual variations of both configurations studied. Equation (11) specifies the configuration (2) from known configuration (1) and known load increments. When the work made by mass and damping forces on virtual displacements du_i is added to Eq. (4), the principle of virtual works for the problem studied is given by

$$\int S_{ij}\, \delta E_{ij}\, dB + \int \rho\, u_i\, \delta u_i\, dB + \int C_i\, u_i\, \delta u_i\, dB - \int T_i\, \delta u_i\, dS - \int P_i\, \delta u_i\, dB = 0, \tag{12}$$

where r and C are mass and damping terms.

The turbulence in the air flow is described by instantaneous wind speed as a function of space and time with mean and fluctuation components given by

$$u(x, y, z, t) = U(x, y, z) + u'(x, y, z), \tag{13}$$

$$v(x, y, z, t) = V(x, y, z) + v'(x, y, z), \tag{14}$$

$$w(x, y, z, t) = W(x, y, z) + w'(x, y, z). \tag{15}$$

The mean values of projections *U*, *V*, *W* are the result of averaging in a certain interval of time the wind speed and the fluctuating components (velocities).

The turbulence scales of the instantaneous wind speed are the measure of the representative dimensions of vortices induced by turbulences inside the air flow. Their importance lies in the fact that they describe the turbulences which "wrap" the plate in a certain time.

The assessment of turbulence motion starts with the specification of the correlation functions of fluctuating components which may be longitudinal, transversal and vertical. In general, the characteristics of the air flow are well defined if the correlation functions are specified for the mean streamwise components longitudinally and transversally. The correlation in time is specified by formulae

$$\rho_{u(i)u(j)}(\tau) = R_{u(i)u(j)}(\tau)/[(\sqrt{(u')^2(t)}).(\sqrt{(u')^2(t+\tau)})], \tag{16}$$

$$R_{u(i)u(j)}(\tau) = u_i(t).u_j(t+\tau) = \lim_{T\to\infty} 1/T \int[u_i(t).u_j(t+\tau)]dt. \tag{17}$$

Eq. (17) represents the covariance function of the process *u* (*t*) being determined by measuring in two different points in space at the difference of time τ (see: Hautoy, C., 1990; Moonen, P., Blocken, B., Carmeliet, J., 2007 and Teleman, E. C., Silion, R., Axinte, E., Pescaru, R., 2008).

According to Taylor´s hypothesis (Hautoy, C., 1990) the inter-correlation between any of the fluctuating parts, discarding the wind instantaneous speed measured in two points being separated by distance Δx in the direction of the wind flow, is equal with the auto-covariance determined for the period studied. The inter-correlation functions give information concerning the dimensions of the turbulences in direction of the wind action. The existence of the mean values of the wind speed inside of turbulent flow is given by the reality that in a certain point i the turbulence has a certain periodicity in time. After a certain period the phenomenon repeats itself in space. These two idioms specify the turbulence scales in time and space. The turbulence scales define frequency of gusts in the wind action. The integral length scales correspond to spatial nature of the wind action specifying the longitudinal, lateral and vertical scales given by

$$L_x = \int \rho_{u'(i)u'(j)}(\Delta x,0,0)\ d(\Delta x), \tag{18}$$

$$L_y = \int \rho_{u'(i)u'(j)}(0,\Delta y,0)\ d(\Delta y), \tag{19}$$

$$L_z = \int \rho_{u'(i)u'(j)}(0,0,\Delta z)\ d(\Delta z), \tag{20}$$

with integration from *0* until ∞. The most important of these three is the longitudinal scale, the other two being practically its derivatives. The integral time scale of the turbulence is defined by

$$\Lambda_T = \int \rho_{u'(i)u'(j)}(\tau)\, d\tau. \tag{21}$$

According to the above Taylor´s hypothesis, the longitudinal scale of a turbulence may be specified by the integral time scale and by the mean wind speed value V in the streamwise direction by

$$L_x = V.\Lambda_T, \tag{22}$$

The studies for determination of the turbulence scale, both at natural scale and in laboratory, have produced the empirical Davenport´s formula

$$\Lambda_T = 0.084\ L/V, \tag{23}$$

given in sec, where L is the longitudinal scale of the in-wind speed and V is the mean wind speed.

In EN 1991-1-4 the integral length scales in wind direction depend on the mean wind velocity U and height z, in accordance with Ref. (Counihan, J.)

The incorporation of the above forcing into behaviour of the flat plate is specified by wave propagation with corresponding interactions and reflexions of laminar and turbulent air flows. The waves initiated are specified by the spectral evolution describing the occurrence of wind turbulences. The spectral evolution is based on the following definitions:

1. Each stationary function $x(t)$ is given in integral form

$$x(t) = \int e^{i\omega t}\, dA(\omega), \tag{24}$$

with symbol $A(\omega)$ for orthogonal complex process studied.

2. Linear transformation $y(t)$ of the function $x(t)$ in Eq. (24) is given by

$$y(t) = \int H(i\omega)\, e^{i\omega t}\, dA(\omega), \tag{25}$$

with $H(\omega)$ as a corresponding admittance function.

3. Spectral densities of functions $x(t)$ and $y(t)$ are connected by

$$S_y(\omega)/S_x(\omega) = |H(i\omega)|^2. \tag{26}$$

Turbulent air flow is defined by a wave number $r_i(w)$, with longitudinal (d) and shear (s) waves. Stationary waves are emitted with complex amplitude $F(w,z_o)$, e.g., $z=z_o$. The wave superposition is given by

$$w_i(t,z) = \int e^{-i\omega t}\, e^{ir\,(\omega z)}\, dF(\omega,z_o). \tag{27}$$

For wave interactions in the turbulences the forcing spectrum is given by $S(\omega,0)$ as function of the response $H(\omega,0)$ to the wind action.

5. Dynamic analysis

The analysis of ultimate behaviour of skew plates subjected to the above forcing is based on the adoption of the Lagrange formulation of motion. The reference state of the plate is incrementally updated during deformation process. The new reference configuration is established at each degree of updated deformation curve of ultimate response of the plate. Incremental form of the equation of motion is given by the analysis of aeroelastic equilibrium of two configurations at time step Δt apart. The increments of laminar and turbulent forcing balance the aeroelastic equilibrium in time $t + \Delta t$ *by*

$$M_t \Delta a_t + C_t \Delta v_t + K_t \Delta u_t = R_{t+\Delta t} - (V_t^I + V_t^D + V_t^S), \tag{28}$$

with inertia forces $V_t^I = M_t a_t$, damping forces $V_t^D = C_t v_t$, stiffness forces $V_t^S = K_t u_t$ and with accelerations, velocities and displacements a_t, v_t, u_t , respectively. The vectors of accelerations and velocities are given by time derivatives of the vector of deformations u_t. The mass, damping and stiffness matrices M_t, C_t and K_t, respectively, are constructed of the element matrices of the plate model studied. The subscript t denotes the actual time and R is the vector of laminar and turbulent forcing. If the system is in equilibrium in time t, then right side of Eq. (28) is identical with the increments of forcing in time step Δt. The increments in displacements, velocities and accelerations are given by increments of forcing and by the matrices of physical properties of the plate studied. If such matrices are variable in time then the validity of Eq. (28) is satisfied only approximately. The approximation error is given by

$$\Delta V_{t+\Delta t} = R_{t+\Delta t} - (V_{t+\Delta t}{}^I + V_{t+\Delta t} + V_{t+\Delta t}), \tag{29}$$

as a measure of the solution accuracy when adopting Eq. (28). Governing incremental equation of motion is then given by modification of Eq. (28) as

$$M_t \Delta a_t + C_t \Delta v_t + P_t \Delta u_t = \Delta R_t, \tag{30}$$

where $P_t \Delta u_t$ is the vector of nonlinear forces. The pseudo-force method (Tesár, 1988), adopted for the solution of the problem, is given by

$$P_t \Delta u_t = K_t \Delta u_t + N_t \Delta u_t - \Delta V_{t+\Delta t}, \tag{31}$$

where $N_t Du_t$ is the vector of aerodynamic nonlinear forces (pseudo-forces) and $\Delta V_{t+\Delta t}$ is the above approximation error. When adopting the pseudo-force technique, the member $P_t \Delta u_t$ is located on the right side of Eq. (30) and the vector of nonlinear forces is applied as the vector of pseudo-forces. In each time step the approximation $N_t \Delta u_t$ is calculated and the iterations run until the term $\Delta V_{t+\Delta t}$ is comparable with the tolerance norm adopted. In the first iteration step as the approximation of $N_t \Delta u_t$ in the first iteration step is given by

$$N_t \Delta u_t = (1 + \beta) N_{t-\Delta t} \Delta u_{t-\Delta t} - \beta N_{t-2\Delta t} \Delta u_{t-2\Delta t}, \tag{32}$$

with β as an extrapolation parameter in scope from 0 until 1.

6. Experiments in aerodynamic tunnel

The testing was made with the model set-up of typical skew flat plate in scale 1:10, developed on the basis of the model similarity with actual structure. The aerodynamic testing was made in the wind tunnel of the Institute of Construction and Architecture of the Slovak Academy of Sciences in Bratislava, Slovakia. Assumed was the type of atmospheric boundary layer suitable for terrain of category II. For testing the modul section with cross-sectional dimensions 1 200 x 1 200 mm and length 6 000 mm was used. Maximal wind velocity obtained was 51 m/s.

The details of experiment, the model similarity with atmospheric boundary layer simulated in the wind tunnel, the model scale of the model and of the wind speed considering the wind direction and intensity of turbulence, etc., are summed up in Ref. (Tesar, A., 2011) The model of the skew flat plate was made of aluminium with dimensions 1 000 x 300 mm and width 4 mm. The plate was supported by steel supports Jäckl 20/20/2 and anchored into the floor of the tunnel. The view of the experimental set-up in the tunnel is in Figure 1.

Figure 1. Side view of the skew plate studied in aerodynamic tunnel

In case of the wind forcing there appear the turbulences on the upper and lower edges of the plate accompanied by wind gusts and local changes of the wind velocity. The wind velocity influences the standard wind pressure being used in the design of the plate. Required was therefore the specification of actual wind velocities appearing on all edges of the skew plate at various wind speeds in aerodynamic tunnel. The speed variations in the wind flow are given by aerodynamic coefficient α

$$\alpha = v_{loc}/v_{ave}, \tag{33}$$

with v_{loc} as a local velocity of turbulent wind flow measured on the edge of the plate and with v_{ave} as an averaged velocity of laminar wind flow in the aerodynamic tunnel. The value v_{ave} corresponds to the standard wind velocity in the given territory and it was used for the design of all structural elements of the skew flat plates studied. The coefficient α specifies the increase of the wind velocity on the edges of the plate. The first goal of experimental testing was therefore the specification of the aerodynamic coefficient α on all edges of the skew plate. The values of coefficient α were adopted for specification of resulting stress and deformation states in the plate. With the data measured the virtual modeling of typical active fields of photovoltaic power plant was made, consisting of a number of skew plates and subjected to wind forcing.

For the measurement of the wind velocities were used the anemometers positioned in the axis of the tunnel (measurement of velocities v_{ave}) as well as on the edges of the skew plate (measurement of velocities v_{loc}). The anemometers for the measurement of velocities v_{loc} were adopted in various positions in order to find the variability of wind velocities on all edges of the plate studied. The time records were made on channels measuring three accelerations *A1*, *A2*, *A3*, four strains *T1*, *T2*, *T3*, *T4* in the centres of all four edges of the skew plate as well as the wind velocities in the tunnel. The accelerations *A1*, *A2* and *A3* were measured on the upper (A1), lower (A2) and side edges (A3) of the plate. The testing was made for:

a) Model in horizontal attitude 0° and located perpendicularly to the direction of the wind flow – the assessment of the shear wind along the plate (Fig. 2).
b) Model in horizontal attitude and turned – 180° compared with the wind flow – the assessment of the air sucking on the plate (Fig. 3).
c) Model in horizontal attitude and turned + 90° compared with the wind flow – the assessment of the wind pressure on the plate (Fig. 4).

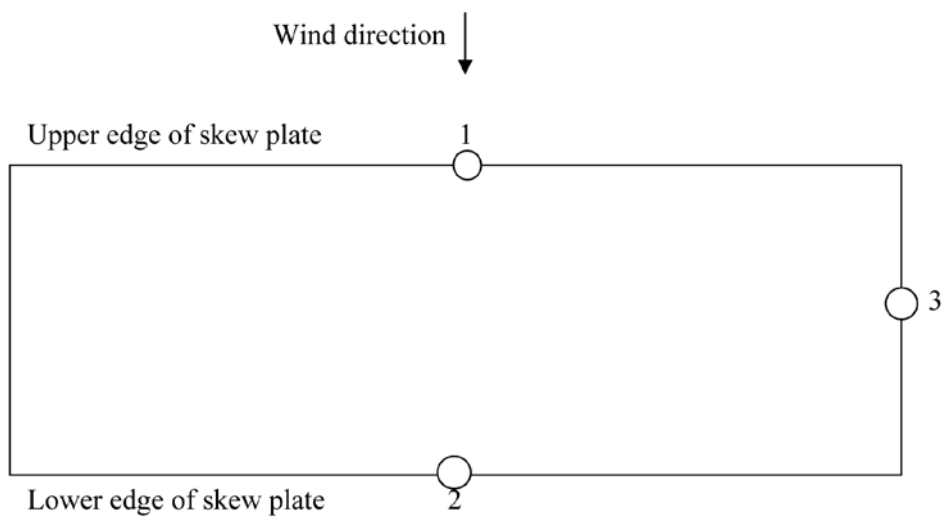

Figure 2. Numbering of measurements in model position 0°

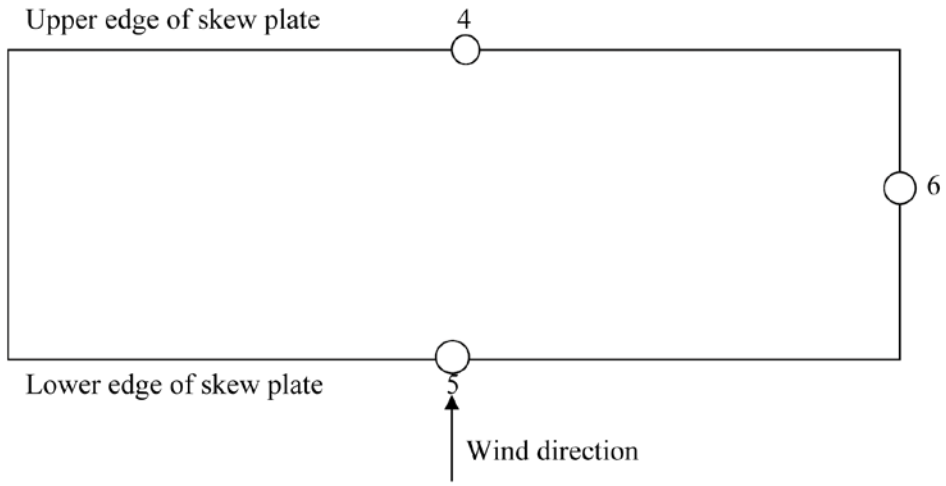

Figure 3. Numbering of measurements in model position – 180°

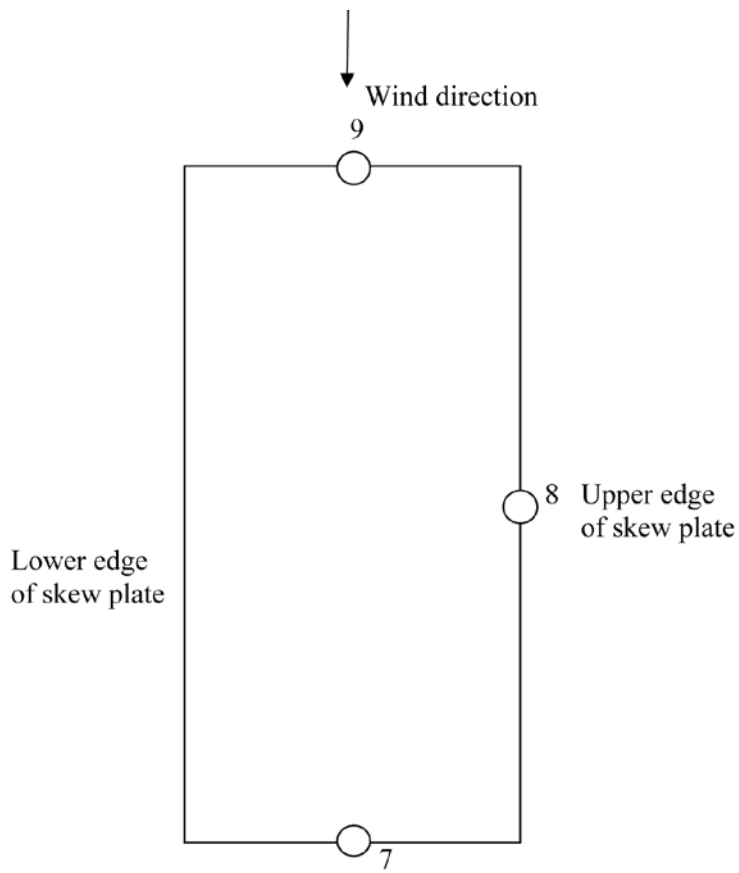

Figure 4. Numbering of measurements in model position + 90°

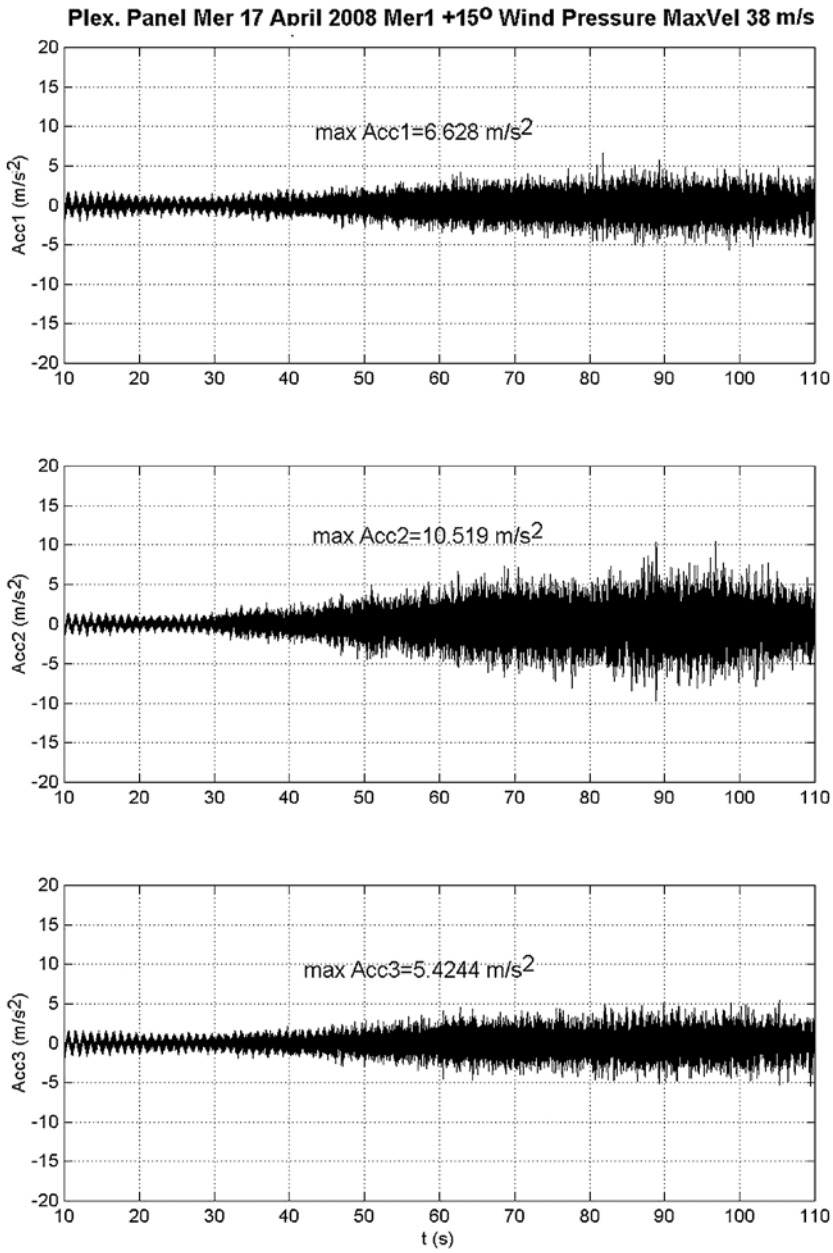

Figure 5. Accelerations *A1*, *A2*, *A3* (upper, lower and side edges of plate) at angle + 90° (wind speed 38 m/s)

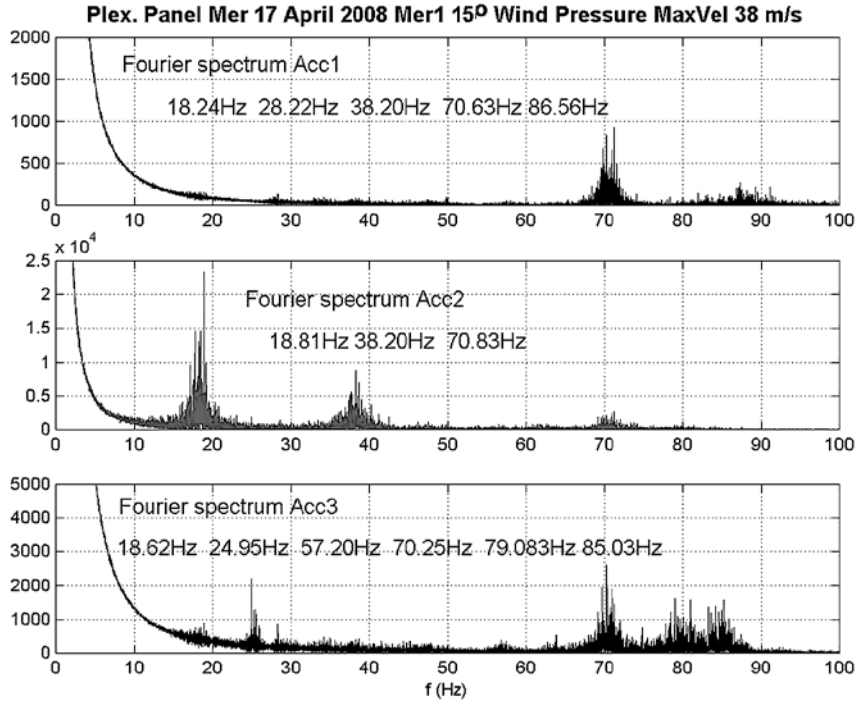

Figure 6. Fourier spectra of accelerations *A1*, *A2*, *A3* (upper, lower and side edges of plate) at angle + 90° (wind speed 38 m/s)

In Figure 5 there are summed up typical accelerations *A1*, *A2*, *A3 (*upper, lower and side edges of plate) at experimental configuration with angle + 90° and by wind speed 38 m/s. In Figure 6 there are typical Fourier spectra of accelerations A1, A2, A3 (upper, lower and side edges of plate) at angle + 90° and by wind speed 38 m/s. In Figure 7 there are typical strains *T1*, *T2*, *T3*, *T4* (upper, lower and side edges of plate) at angle + 90° and by wind speed 38 m/s.

In accordance with the measurements made in critical points (see Figs. 2 – 4) and summed up in Tables 1 – 3 it was stated, that response of the plate is dominated by deformations with turbulent components of pressure and sucking of wind which are irregularly distributed along the surface of the plate. Turbulent wind flows initiated the ultimate aeroelastic response of the plate.

The values of aerodynamic coefficient α, obtained in aerodynamic tunnel, are summed up in Tables 1 – 3. The tables contain the wind speeds on the edges of skew plate, specified in scope of measurements 1 until 9 at various wind speeds. In tables there are summed up the automatically established wind speeds 10 – 50 m/s in the aerodynamic tunnel, averaged actual wind speeds v_{ave} in the wind tunnel as well as the local wind speeds v_{loc} on all edges of the plate. In tables there are also the aerodynamic coefficients $\alpha = v_{loc}/v_{ave}$ on all edges of the plate. In Table 3 there is also the comparison of measured and calculated values of the coefficient α.

The averaged increase of speeds and pressures of wind flows on the upper, lower and side edges of the plate are given by aerodynamic coefficients α = 1.4255, 1.6532 and 1.4080, respectively. The averaged increase of the wind pressure on the plate due to the change of the wind direction and due to the turbulences appearing is given for wind sucking by multiplicator – 1.65 and for the wind pressure by multiplicator 1.43 of the standard values valid for the face action of the wind on the model.

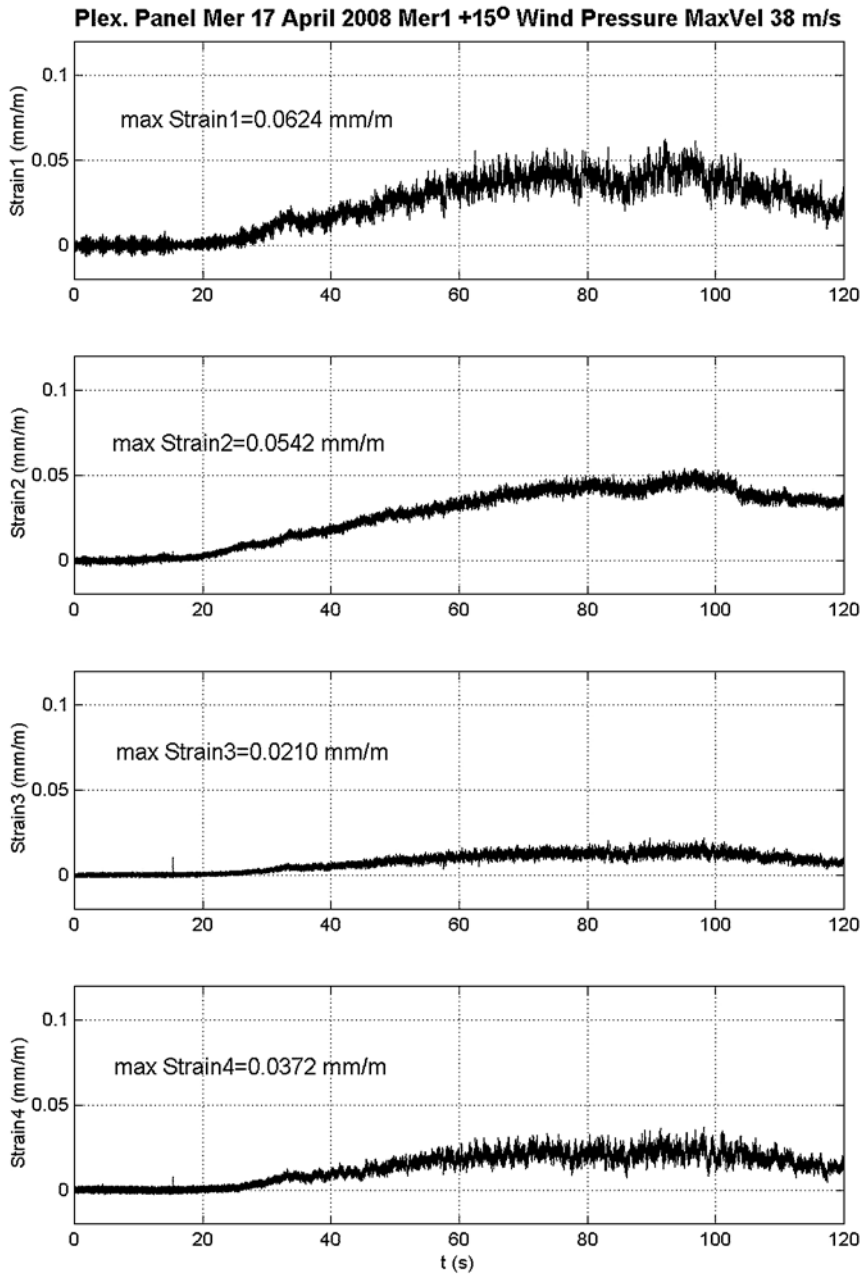

Figure 7. Strains *T1*, *T2*, *T3*, *T4* (upper, lower and side edges of plate) at angle + 90° (wind speed 38 m/s)

Due to appearance of the wind gusts the ultimate response of the model was initiated. There appeared combined axial and shear amplitudes of vibration parallel with the plane of the skew plate.

Table 1. Results of measurements Nr. 1, 2 and 3

Wind speed [m/s]	Measu-rement Nr. 1 v_{loc} [m/s]	Measu-rement Nr. 1 v_{ave} [m/s]	Measu-rement Nr. 1 $\alpha=v_{loc}/v_{ave}$	Measu-rement Nr. 2 v_{loc} [m/s]	Measu-rement Nr. 2 v_{ave} [m/s]	Measu-rement Nr. 2 $\alpha=v_{loc}/v_{ave}$	Measu-rement Nr. 3 v_{loc} [m/s]	Measu-rement Nr. 3 v_{ave} [m/s]	Measu-rement Nr. 3 $\alpha=v_{loc}/v_{ave}$
10	14.5	10.1	1.4356	18.8	10.1	1.8614	15.8	10.1	1.5643
20	28.8	20.2	1.4257	35.6	20.2	1.7624	30.6	20.2	1.5148
30	39.9	30.1	1.3256	48.9	30.1	1.6249	42.9	30.1	1.4252
40	51.4	40.1	1.2817	59.7	40.1	1.4888	55.7	40.1	1.3890
50	65.2	50.2	1.2988	74.8	50.2	1.4900	69.8	50.2	1.3904

Table 2. Results of measurements Nr. 4, 5 and 6

Wind speed [m/s]	Measu--rement Nr. 4 v_{loc} [m/s]	Measu-rement Nr. 4 v_{ave} [m/s]	Measu-rement Nr. 4 $\alpha=v_{loc}/v_{ave}$	Measu-rement Nr. 5 v_{loc} [m/s]	Measu-rement Nr. 5 v_{ave} [m/s]	Measure-ment Nr. 5 $\alpha=v_{loc}/v_{ave}$	Measu-rement Nr. 6 v_{loc} [m/s]	Measure-ment Nr. 6 v_{ave} [m/s]	Measu-rement Nr. 6 $\alpha=v_{loc}/v_{ave}$
10	13.5	10.1	1.3366	18.8	10.1	1.9603	14.0	10.1	1.7129
20	26.8	20.2	1.3267	34.6	20.2	1.8119	27.5	20.2	1.5742
30	36.9	30.1	1.2259	47.9	30.1	1.6578	40.9	30.1	1.3588
40	49.4	40.1	1.2319	56.7	40.1	1.4638	52.7	40.1	1.4389
50	61.2	50.2	1.2191	66.8	50.2	1.4103	63.8	50.2	1.3506

Table 3. Resuls of measurements Nr. 7, 8 and 9 together with calculated vales of α (in brackets)

Wind speed [m/s]	Measu-rement Nr. 7 v_{loc} [m/s]	Measu-rement Nr. 7 v_{ave} [m/s]	Measu-rement Nr. 7 $\alpha=v_{loc}/v_{ave}$	Measu-rement Nr. 8 v_{loc} [m/s]	Measu-rement Nr. 8 v_{ave} [m/s]	Measu-rement Nr. 8 $\alpha=v_{loc}/v_{ave}$	Measu-rement Nr. 9 v_{loc} [m/s]	Measu-rement Nr. 9 v_{ave} [m/s]	Measu-rement Nr. 9 $\alpha=v_{loc}/v_{ave}$
10	13.7	10.1	1.3564 (1.3762)	17.8	10.1	1.7623 (1.8142)	14.3	10.1	1.4158 (1.4833)
20	26.8	20.2	1.3267 (1.3341)	36.6	20.2	1.8119 (1.8231)	28.7	20.2	1.4208 (1.4471)
30	38.9	30.1	1.2923 (1.3026)	49.9	30.1	1.6578 (1.8452)	40.4	30.1	1.3422 (1.3610)
40	52.4	40.1	1.3067 (1.3161)	60.7	40.1	1.5137 (1.5338)	52.6	40.1	1.3117 (1.3275)
50	66.2	50.2	1.3187 (1.3228)	76.8	50.2	1.5299 (1.5730)	67.7	50.2	1.3488 (1.3722)

7. Conclusions

On the basis of evaluation of the virtual results obtained in the whole active fields of the photovoltaic power plants it has been found, that ultimate displacement and stress states appear in boundary regions of the fields, where the wind flows have distinctly turbulent character. In real structures such regions are created by boundary strips having the width of 3m along the periphery of the field studied.

Acknowledgements

The authors are indebted to the representatives of the enterprise RAAB VILLANZSZERELŐ KFT., CSÖRGŐFA SOR 6, 9027 GYŐR, for cooperation by preparation of this report.

References

[1] Bleich, F. (1950), "The Flutter Theory", Ch. 7 of Bleich, F., mcCullough, C. B., Rosecrans, R. and Vincent, G. S. The mathematical theory of vibration in suspension bridges. United States Government Printing Office, Washington, 241-281.

[2] Counihan, J. (1961), "Adiabatic atmospheric boundary layers, a review and analysis", Atmos. Environment 9, 879-905.

[3] Curami, A. and Zasso, A. (1993), Extensive identification of bridge deck aeroelastic coefficients, average angle of attack, Reynolds number and other parameter effects. ProWE III, Hong Kong.

[4] Davenport, A. G. (1962), "Buffeting of a suspension bridge by storm winds", ASCE journal of Structures Division 88, 233-264.

[5] Diana, G., Bruni, S., Cigada, A. and Collina, A. (1993), "Turbulence effect on flutter velocity in long span suspended bridges", Journal of Wind Engineering and Industrial Aerodynamics 48, 329-342.

[6] Diana, G., Chelli, F., Collina, A., Zasso, A. and Bruni, S. (1998), Aerodynamic design of long span suspension bridges, IABSE Symposium, Kobe.

[7] Diana, G., Chelli, F., Zasso, A. and Bocciolone, M. (1999), "Suspension bridge response to turbulent wind. Comparison of a new numerical simulation method results with full scale data", Proc. of 10th International Conference on Wind Engineering, Copenhagen.

[8] Frandsen, A. G. (1966), "Wind stability of suspension bridges", paper 43 of International Symposium on Suspension Bridges, Proceedings. Laboratório Nacional de Engenharia Civil, Lisboa, 609-627.

[9] Hautoy, C. (1990), Simulation des proprietes dynamiques du vent. Souflerie a couche limite du C.S.T.B., Nantes, France.

[10] Juhásová, E., Motlík I. and Vrabec, M. (1998), "Some experiences with calibration and modeling in wind tunnel of ICA SAS", Building Research journal 46, 47-69.

[11] Klöppel, K. and Weber, G. (1963), "Teilmodellversuche zur Beurteilung des aerodynamischen Verhaltens von Brücken", Der Stahlbau 4, 113-121.

[12] Larose, G. L., Davenport, A. G. and King, J. P. C. (1992), "Wind effects on long span bridges. Consistency of wind tunnel results", Journal of Wind Engineering and Industrial Aerodynamics 41-44, 1191-1202.

[13] Miyata, T., Yamada, K., Kanazaki, T. and Iijima, T. (1992), "Construction of boundary layer wind tunnel for long-span bridges", Journal of Wind Engineering and Industrial Aerodynamics 41-44, 885-889.

[14] Moonen, P., Blocken, B. and Carmeliet, J. (2007), "Indicators for the evaluation of wind tunnel test section flow quality and application to a numerical closed circuit wind tunnel", Journal of Wind Engineering and Industrial 95, 1289-1314.
[15] Rocard, Y. (1965), "Instabilité des ponts suspendus dans le vent – expériences sur modéle réduit", Paper 10 of Wind Effects on Buildings and Structures. H.m.S.O., London, vol. II, 434-459.
[16] Scanlan, R. H. and Tomko, J. J. (1971), "Airfoil and bridge deck flutter derivatives", ASCE journal of Engineering mechanics 97, 1717-1737.
[17] Scanlan, R. H., Béliveau, J. G. and Budlong, G. (1974), "Indicial aerodynamics functions for bridge decks", ASCE journal of Engineering mechanics 100, 657-672.
[18] Scanlan, R. H., Jones, N. P. and Singh, L. (1971), "Inter-relations among flutter derivatives", Journal of Wind Engineering and Industrial Aerodynamics 69-71, 829/837.
[19] Scruton, C. (1965), "Discussion. Wind Effects on Buildings and Structures", H.m.S.O., London, vol. II, 555-556.
[20] Sears, R. W. (1941), "Some aspects of non-stationary airfoil theory and its practical application", Journal of Aeronautical Sciences 8, 104-108.
[21] Selberg, A. (1961), "Oscillation and aerodynamic stability of suspension bridges", Acta P. 308, Ci. 13, 43-54.
[22] Selberg, A. and Hjorth-Hansen, E. (1966), "Aerodynamic stability and related aspects of suspen sion bridges", paper 20 of International Symposium on Suspension Bridges, Proceedings. Laboratório Nacional de Engenharia Civil, Lisboa, 361-366.
[23] Simiu, E. and Scanlan, R. H. (1996), Wind Effects on Structures. Wiley-Interscience, New York.
[24] STN EN 1991-1-4 Eurocode 1. Structural loads. Part 1.4. General loads. Wind loads.
[25] Tanaka, H. (1992), "Similitude and modeling in bridge aerodynamics", Larsen (ed.): Aerodynamics of Large Bridges, Balkema, Rotterdam.
[26] Teleman, E. C., Silion, R., Axinte, E. and Pescaru, R. (2008), "Turbulence scales simulations in atmospheric boundary layer wind tunnels", Bulletinul Institutului Polytehnic din Iasi, Publicat de Universitatea Tehnica "Gheorghe Asachi" din Iasi, Tomul LIV (LVIII), Fasc. 2, 7-14.
[27] Tesar, A. (1978), Aeroelastic Response of Transporter Shell Bridges in Smooth Air Flow. The Norwegian Institute of Technology, Tapir, Trondheim.
[28] Tesar, A. (1988), Transfer matrix method. KLUWER Academic Publishers, Dordrecht, Boston, London.
[29] Tesar, A. (2011), Aeroelastic Assessment of Elements of Photovoltaic Power Plants. Technical Report for RAAB VILLANZSZERELŐ KFT., CSÖRGŐFA SOR 6, 9027 GYŐR, Institute of Construction and Architecture, Slovak Academy of Sciences, Bratislava.
[30] Tesar, A. and Svolik, J. (1993), "Wave distribution in fibre members subjected to kinematic forcing", Int. journal for Communication in Numerical mechanics 9.
[31] Tesar, A. and Tvrda, K. (2006), "Energy approach for analysis of nonlinear time response", Building Research journal 54, 101-122.
[32] Tesar, A. and Tvrda, K. (2007), "Energy approach for solution of nonlinear natural vibration", Building Research journal 55, 71-84.
[33] Theodorsen, T. (1935), General theory of aerodynamic instability and the mechanism of flutter. Report 496, U.S. Advisory Committee for Aeronautics, Langley, VA, U.S.A.